Analysis for Microseismic Energy of Immediate Rockbursts in Deep Tunnels with Different Excavation Methods

Yang Yu[1]; Bing-rui Chen[2]; Chang-jie Xu[3]; Xin-hong Diao[4]; Li-hong Tong[5]; and Yu-feng Shi[6]

Abstract: This study integrates microseismic data and data from hundreds of rockbursts of different intensities that occurred in a water drainage tunnel and four deep headrace tunnels at Jinping II Hydropower Station in Sichuan Province, China. The tunnels with overburden depths between 1,900 and 2,525 m, the maximum principal stress of which reaches 63 MPa in a rock mass, is composed mainly of marble. The tunnels have a total length of 12.4 km. The microseismic energy produced during the development of immediate rockbursts induced by the excavation by the drill-and-blast method (DBM) and a tunnel-boring machine (TBM) were studied. The results indicate that the daily maximum microseismic energy can be used as a basis for estimating rockburst intensity. The daily maximum microseismic energy (logarithm) corresponds to intense rockbursts (>6), moderate rockbursts (between 5 and 6), weak rockbursts (between 4 and 5), and no rockbursts (<4). Before the occurrence of intense rockbursts, there were numerous weak and moderate rockbursts during TBM excavation, whereas such a phenomenon was not observed during DBM excavation. The microseismic energy (logarithm) primarily concentrated in the range of 1 to 5 under TBM excavation, which is concentrated in the range of –1 to 4 under DBM excavation. For rockbursts of the same intensity, the range of microseismic energy remained the same for either type of excavation method. The distribution range of the microseismic energy moved in the direction of high energy as the level of rockburst intensity rose (intense rockbursts > moderate rockbursts > weak rockbursts > no rockburst). Microseismic energy can be used as a guideline for building a warning system and reduce the risk of rockbursts during construction. **DOI: 10.1061/(ASCE)GM.1943-5622.0000805.** © *2016 American Society of Civil Engineers.*

Author keywords: Drill-and-blast method (DBM); Tunnel-boring machine (TBM); Immediate rockburst; Microseismic events; Microseismic energy; Rockburst intensity.

Introduction

Rockbursts occur frequently in deep hard-rock tunnels during tunnel construction, and they can cause safety problems, construction delays, and economic losses. For example, hundreds of rockbursts were observed during the excavation of a drainage tunnel, four headrace tunnels, and two assistant tunnels in the Jinping II Hydropower Station in Sichuan Province, China, and caused billions of yuan (¥) in economic loss and more than 100 casualties (Tang 2000; He et al. 2010; Zhang et al. 2012a; Feng et al. 2013).

Rockbursts in deep tunnels can be categorized as time-delay or immediate rockbursts on the basis of their time of occurrence. The former occur several days or several months after excavation, with interrupted occurrences of microseismicity. However, the latter occurs between 0 and 30 m from the working face within a few hours to several days after excavation, and microseismicity occurs continuously (Chen et al. 2012). In deep hard-rock tunnels, most rockbursts are immediate. These immediate rockbursts are studied in this paper. Immediate rockbursts in diversion tunnels of the Jinping II Hydropower Station were divided into three levels of intensity (weak, moderate, and intense) on the basis of the sound, shape, and failure features of the rockbursts (Tang 1992; Wang et al. 1999), as shown in Table 1.

In the high-stress conditions during TBM and DBM excavation, the stress path and extent of damage are different. The initial in-situ stress of the working face is a static unloading stress field during the TBM excavation, and the elastic strain energy stored in the rock mass is released gradually (Barton 2000; Li et al. 2007; Eshragi and Zare 2015). However, in DBM excavation, the initial in-situ stress is a dynamic unloading stress field, and the damage to the surrounding rock caused by the dynamic unloading stress wave is produced near the working face (Cook et al. 1966; Abuov et al. 1988). Cai (2008) considered DBM excavation to mean that transient unloading and instantaneous blasting can produce large quantities of unbalanced force. Under such circumstances, part of the strain energy is transformed into kinetic energy, which must be released in the process of stress adjustment. This is quite different from TBM excavation, in which the stress is static unloading. Yan et al. (2011) also found that the stress paths during TBM (static unloading stress fields) and DBM (dynamic unloading stress fields) excavation in deep tunnels are different. Hence, there is a need to distinguish between the two in excavation engineering and geomechanics research.

[1]Lecturer, College of Civil Engineering and Architecture, East China Jiaotong Univ., Nanchang 330013, China (corresponding author). E-mail: lukeryuyang@163.com

[2]Professor, State Key Laboratory of Geomechanics and Geotechnical Engineering, Institute of Rock and Soil Mechanics, Chinese Academy of Sciences, Wuhan 430071, China.

[3]Professor, College of Civil Engineering and Architecture, East China Jiaotong Univ., Nanchang 330013, China.

[4]Professor, College of Civil Engineering and Architecture, East China Jiaotong Univ., Nanchang 330013, China.

[5]Lecturer, College of Civil Engineering and Architecture, East China Jiaotong Univ., Nanchang 330013, China.

[6]Lecturer, College of Civil Engineering and Architecture, East China Jiaotong Univ., Nanchang 330013, China.

Note. This manuscript was submitted on March 24, 2016; approved on August 2, 2016; published online on October 6, 2016. Discussion period open until March 6, 2017; separate discussions must be submitted for individual papers. This paper is part of the ***International Journal of Geomechanics***, © ASCE, ISSN 1532-3641.

Stress waves generated by the process of rock mass failure are called microseismic. They can be detected by seismic instruments. Analyzing and processing these microseismic waves can determine size, time, space, energy, and other information about the microfracturing that occurs in the process of rock mass failure. Microseismic monitoring has been applied successfully during the construction of deep tunnels (Tang et al. 2009; Feng et al. 2013; Rutqvist and Rinaldi 2013). Microseismic energy is one of the most important parameters used to describe the size of microseismic events (Chen et al. 2015). This paper focuses on the relationship between the microseismic energy and rockbursts that result from two different excavation methods, TBM and DBM, in deep tunnels. The relationship between rockburst intensity and the daily maximum microseismic energy events is studied. The distribution range of microseismic energy in the evolutionary process of rockbursts of different intensities involves contrastive analysis. Few studies have explored these processes, and this study addresses that gap.

Project Introduction and Microseismic Monitoring

Project Introduction

In this paper, the authors use as a case study the Jinping II Hydropower Station, which is located on the Yalong River in Sichuan Province in southwest China. Fig. 1 shows the geographical

Table 1. Intensities of Immediate Rockbursts in Deep Tunnels of the Jinping II Hydropower Station

Intensity of rockburst	Main failure type	Sound	Depth of failure (m)	Construction affected
Weak	Slight spalling and slabbing in surface of surrounding rock mass; rock mass was not ejected	Cracking sound was heard occasionally	<0.5	Barely affected
Moderate	Severe spalling and slabbing of surrounding rock mass; rock mass was slightly ejected	Cracking sound like a detonator blast; slight cracking sound lasted for some time inside the rock mass	>0.5 and <1.0 (failure range was obvious)	Affected to some extent
Intense	Great deal of rock mass was ejected suddenly with great power	Failure sounded like an explosive blast; it was loud and lasted longer	>1.0 (failure range was extensive)	Seriously affected

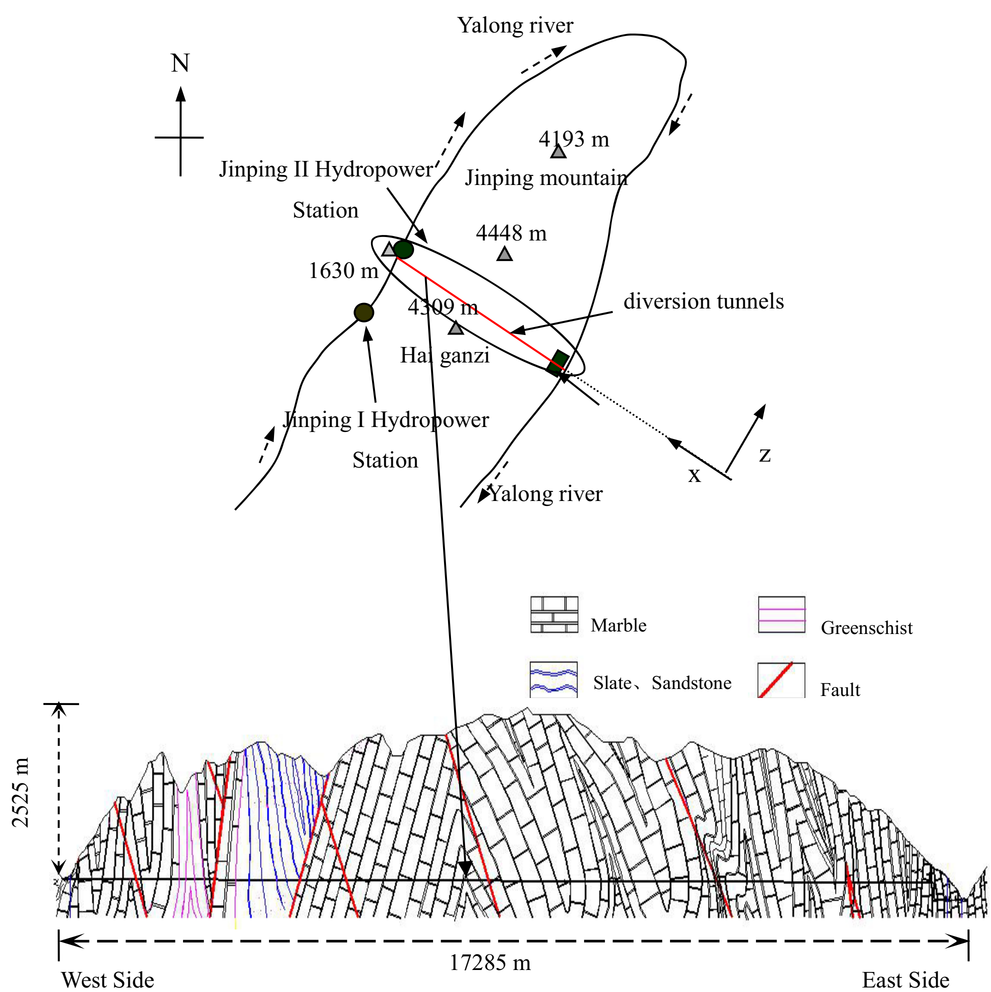

Fig. 1. Location and geological section of diversion tunnels for the Jinping II Hydropower Station (data from Feng et al. 2013)

location and geological section of diversion tunnels in the Jinping II Hydropower Station, the lengths of which are approximately 17.3 km on average (Feng et al. 2013).

The rock surrounding the diversion tunnels is mainly composed of category II and III marble (Poisson's ratio is 0.21–0.33, maximum principal stress is 46–73 MPa, compressive strength is 55–114 MPa, elasticity modulus is 25–40 GPa, and modulus of deformation is 8–16 GPa) (Zhang et al. 2012a). The length of the tunnels that are covered by a rock mass with a thickness greater than 1,500 m is approximately 75%, and the maximum buried depth of these tunnels is 2,525 m (Feng et al. 2013).

Real-Time Microseismic Monitoring of the Rockburst-Development Process

Microseismic monitoring took place on the five diversion tunnels, the four headrace tunnels, and the drainage tunnel. TBM excavation (No. 3 headrace tunnel chainage K10 + 049∼11+165) and DBM excavation (No. 1, 2, 3, and 4 headrace tunnels and the drainage tunnel) were both used in the course of construction, as shown in Fig. 2. The construction process indicated that rockbursts occurred frequently with primarily weak-to-moderate intensity, caused significant safety problems, and, in local areas, even intense rockbursts occurred (Feng and Zhou 2006; Zhang et al. 2012b).

The adopted microseismic monitoring system was constructed on the basis of the South African Integrated Seismic System (ISS). Two groups of microseismic sensors were installed behind the working face, and the seismic data acquisition unit and microseismic sensors were moved forward as the tunnel face advanced. The system was designed to maintain a reasonable distance between the sensors and the working face to ensure the personal safety of personnel during its installation and to prevent damage to the equipment caused by blasting. On this basis, a real-time microseismic monitoring method was established for a deep tunnel as follows: first, a row of microseismic sensors (numbered D1-1 to D1-4) was installed 110 m behind the working face; then, a second row (numbered D2-1 to D2-4) was installed 40 m in front of the first row (i.e., 70 m behind the working face). Sensors D1-2 and D2-3 were acceleration sensors; the others were velocity sensors. The drill-hole depth for sensor installation was 3 m, as shown in Figs. 3(a and b). As the tunnel excavation proceeded, when the working face was 150 m in front of the first row of sensors (i.e., 110 m in front of the second row), the sensors in the first row were recycled and reinstalled some 40 m in front of the second row (i.e., 70 m behind the working face). The procedure was repeated as required. In the end, eight channels were allocated to the two rows: the first and second rows were 110–150 and 70–110 m, respectively, from the working face in this deep tunnel, as shown in Fig. 3(c). Moreover, the spatial layout of the microseismic sensors was deemed reasonable, and different types of sensors working cooperatively can improve positioning accuracy more effectively. Microseismic information on hundreds of rockbursts has been recorded by real-time microseismic monitoring systems (Feng et al. 2015).

Characteristics of Microseismic Energy Induced by Immediate Rockbursts

Energy of Microseismic Events

There are many cracks generated during the evolution of a rockburst. During rock mass failure, rockbursts radiate energy in the form of a stress wave (Savoikar and Choudhury 2012; Chattopadhyay et al. 2014) for each microseismic event. These microseismic events, which are caused by elastic deformation becoming inelastic, can be received by seismic recording instruments. Feng et al. (2015) suggested a method for describing the changes in a rock mass before rockbursts by collecting

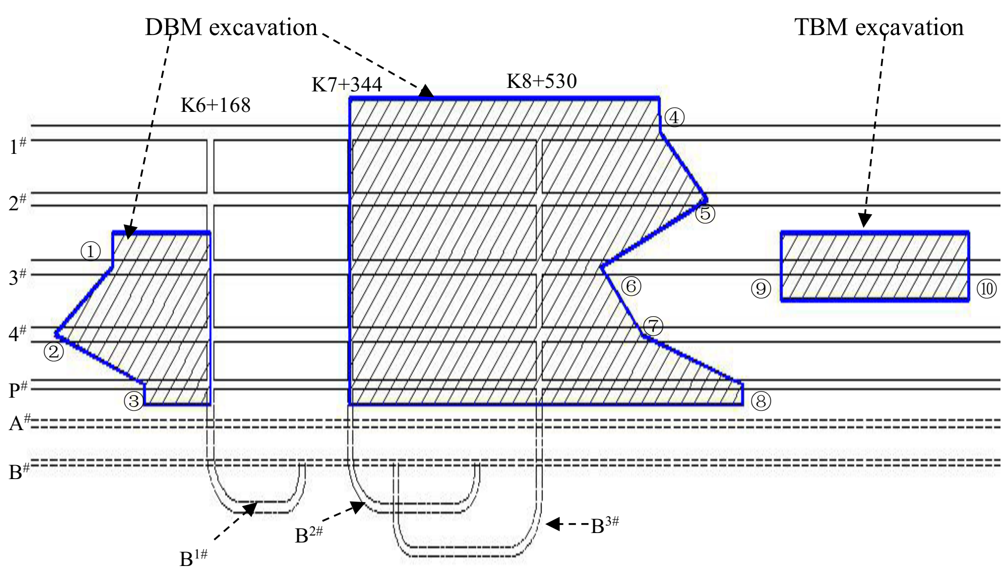

Fig. 2. Ranges of microseismic monitoring of TBM and DBM excavation of diversion tunnels for the Jinping II Hydropower Station (Note: 1#, 2#, 3#, and 4# are the indexes of the four headrace tunnels; P# is the drainage tunnel; A# and B# are traffic tunnels; and B1#, B2#, and B3# are branches of traffic tunnel B# that were used to accelerate the construction of the four headrace tunnels; units are meters)

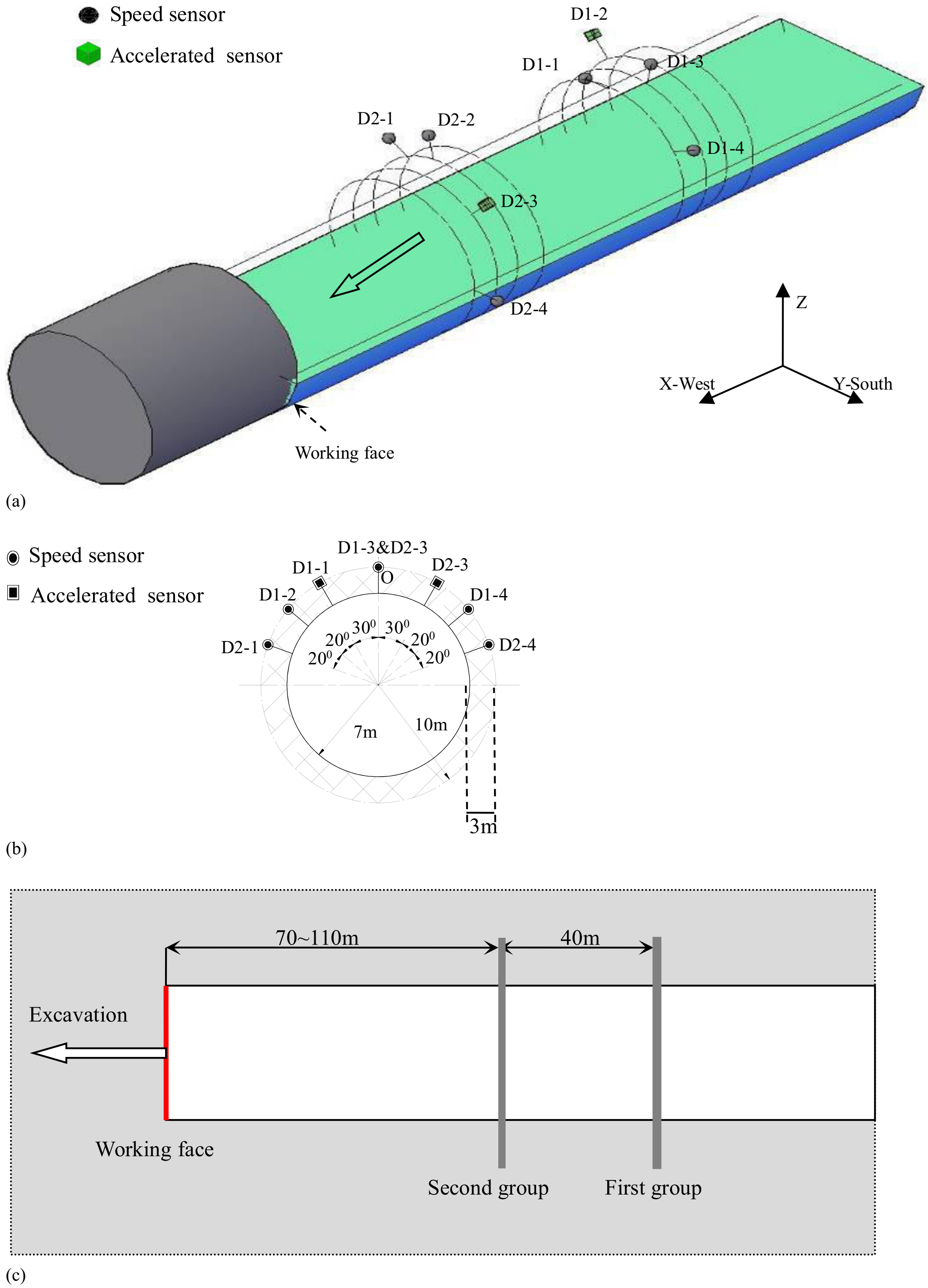

Fig. 3. Real-time microseismic monitoring method in a deep tunnel: (a) distribution of sensors; (b) section distribution of sensors; (c) sensor distribution plan

the information of microseismic events that happened during rockbursts.

Fig. 4 shows a waveform from a microseismic source during crack generation in a rock mass. According to the velocities of the P wave and the S wave, and the difference in their arrival times, the distance R from the microseismic source to each sensor was known. The location of the microseismic event is determined from the eight channels shown in Fig. 3(a). The energy released can be received and computed by the installed microseismic monitoring instruments (Mendecki et al. 1999) as

$$E_P = \frac{8}{5}\pi p v_p R^2 \int_0^{t_s} u_{\mathrm{corr}}^2(t)dt \tag{1}$$

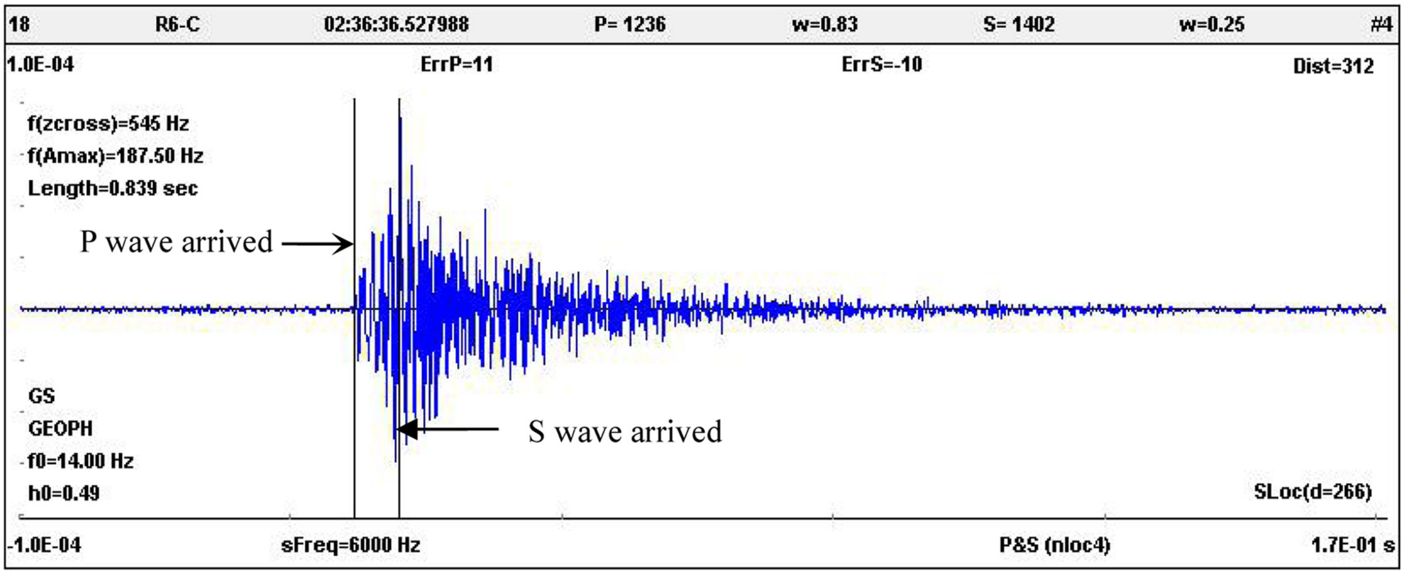

Fig. 4. Waveform of a typical microseismic source

$$E_S = \frac{8}{5}\pi p v_s R^2 \int_0^{t_s} u_{\text{corr}}^2(t)dt \tag{2}$$

where $E_{P,\,S}$ (E_P plus E_S) = energy released from the microseismic event averaged across the eight installed channels (called *microseismic energy* here); p = density of the rock; $v_{p,s}$ = velocity of the P wave and S wave; t_s = duration; and $u_{\text{corr}}(t)$ = coefficient for correcting far-field velocity.

Occurrence of Immediate Rockbursts

An intense rockburst with a loud sound like blasting occurred at the northern sidewall of the No. 3 headrace tunnel at chainage K11+041∼049 at approximately 4:00 p.m. on September 9, 2010, during TBM excavation. The surrounding rock was coarse-grained white marble T2b with no geological structural planes. The failure pit of the rockburst was approximately 1.4 m deep, 8 m wide, and 9 m high. The surface of the rockburst pit is shown in Fig. 5(a). Microseismic events that happen between 10 m ahead of and 30 m behind the working face [Fig. 5(b)] have an impact on rockbursts and were selected as a warning of immediate rockbursts (Feng et al. 2013). This range was used for investigating the rockburst. The microseismic events monitored in the zone (10 m ahead of and 30 m behind the working face) [Fig. 5(b)] were selected for study of the rockburst. The spatial distribution of microseismic events in this zone during the development of the rockburst on September 9, 2010, is shown in Fig. 5(b). It can be seen that the maximum and minimum microseismic energies (logarithmic) are 6.33 and 1.10, respectively.

At approximately 11:00 a.m. on April 28, 2011, an intense immediate rockburst occurred in the south wall of the No. 4 headrace tunnel at chainage K5+722∼734 during DBM excavation. The failure pit of the rockburst was approximately 1.2 m deep, 11.4 m wide, and 8.5 m high, and the surface of the rockburst pit was rough, as illustrated in Fig. 6(a). A moderate rockburst occurred in the north wall at chainage K6+062∼068 in the drainage tunnel at approximately 4:00 a.m. on August 16, 2011. The pit of the rockburst [shown in Fig. 6(b)] was approximately 0.7 m deep, 6.2 m wide, and 5.1 m high. A large number of rockbursts that occurred in the Jinping II Hydropower Station are not listed.

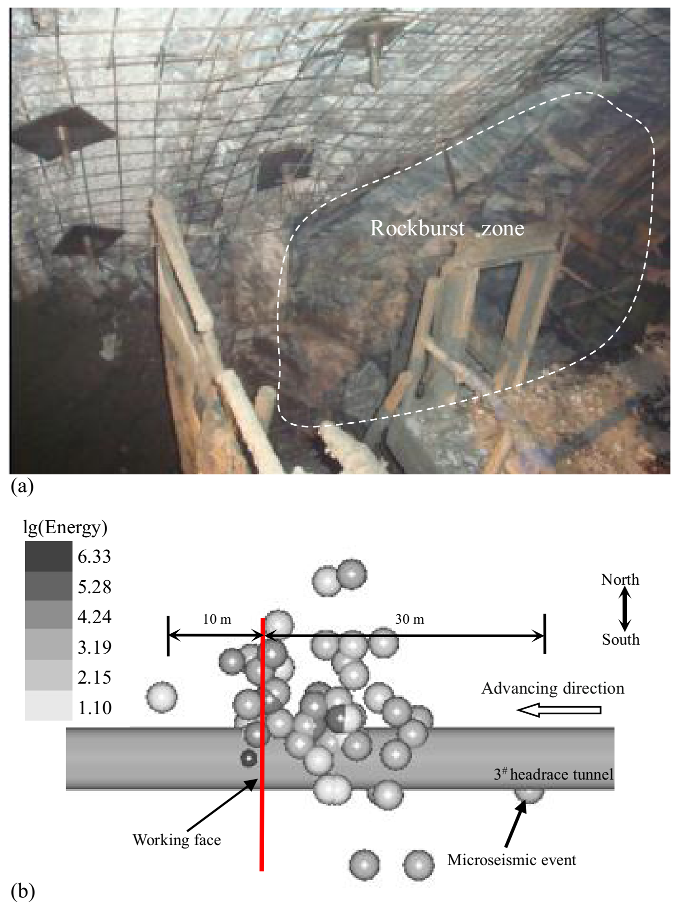

Fig. 5. (a) After the intense rockburst in the No. 3 headrace tunnel on September 9, 2010 (image by authors); (b) microseismic events of the rockburst

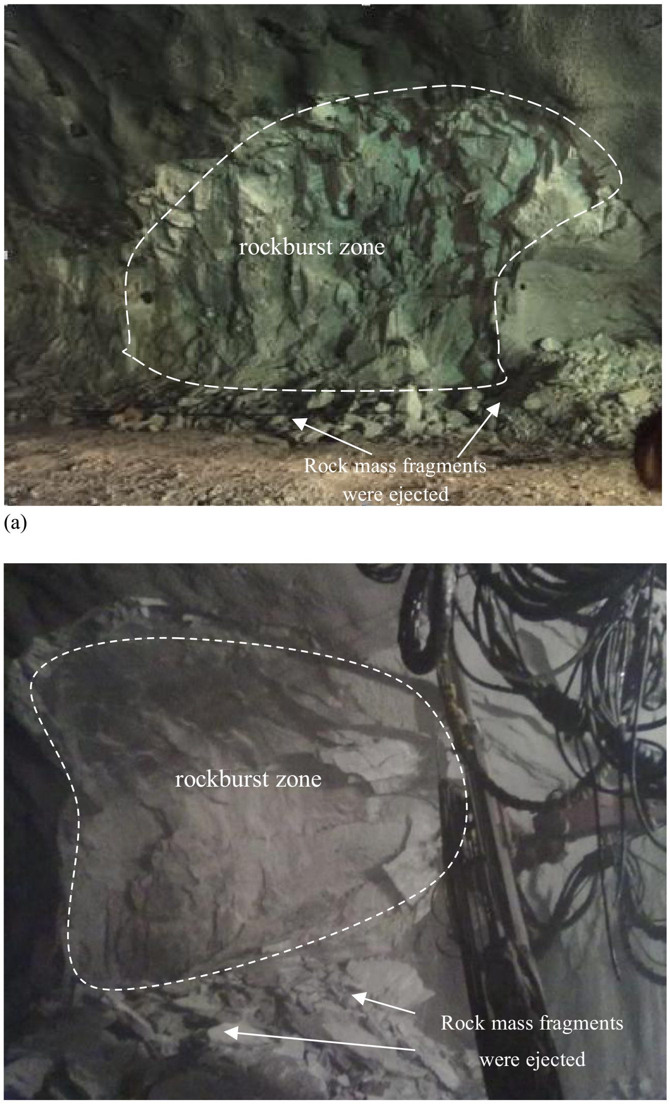

Fig. 6. Rockbursts in the No. 3 headrace tunnel on (a) April 28, 2011, and (b) August 16, 2011 (images by authors)

Relationship between Microseismic Energy and Intensity of Immediate Rockburst during TBM Excavation

A large number of microseismic events were produced during the evolution of the rockbursts on the basis of fracture mechanics. If the process of cracking is static, it will not release energy. However, if the crack produced propagates rapidly, it will release more energy and be more harmful to the engineering. Thus, study of the evolutionary characteristics of maximum-energy microseismic events during the process of deep tunnel excavation is important in guiding the establishment of a dynamic warning system to reduce the risk of rockbursts during construction.

No. 3 headrace tunnel chainage K10+676-11+165 (Fig. 2), with overburden depths between 1,972 and 2,029 m and lengths of 589 m, was excavated by a TBM (July 31 to September 19, 2010). The surrounding rock (which had good integrity, Karst nondevelopment, and moderate amounts of groundwater) is composed mainly of marble. Fig. 7 shows the relationship between rockburst intensity and daily maximum-energy microseismic events in the warning zone, and Table 2 shows the occurrence time and energy release (logarithm) of the typical rockburst in this excavation section. It can be seen in Fig. 7 and Table 2 that the energy released from the rockburst events is the maximum, and the daily microseismic events with maximum energy along the working face can be used for estimating the immediate rockburst intensity. The daily maximum microseismic energy (logarithm) in intense rockbursts is >6; in moderate rockbursts, it ranges from 5 to 6, in weak rockbursts, it ranges from 4 to 5, and when there is no rockburst, it is <4. Before the occurrence of intense rockbursts, numerous weak and moderate rockbursts occurred in the warning zone during TBM excavation. On September 5, there were no rockbursts, whereas from September 6 to 8, weak rockbursts occurred frequently (three times per day on September 6, and increased to 11 times per day on September 8, until an intense rockburst occurred on September 9, as shown in Fig. 8).

Energy was released by the surrounding rock step by step during the TBM excavation. A large number of rockbursts of different intensities occurred frequently in the same range. Before the occurrence of intense rockbursts, there were numerous weak and moderate rockbursts (before moderate rockbursts, there are often weak rockbursts also). Therefore, to reduce (or prevent) intense rockbursts and ensure security and efficiency in deep hard-rock tunnels

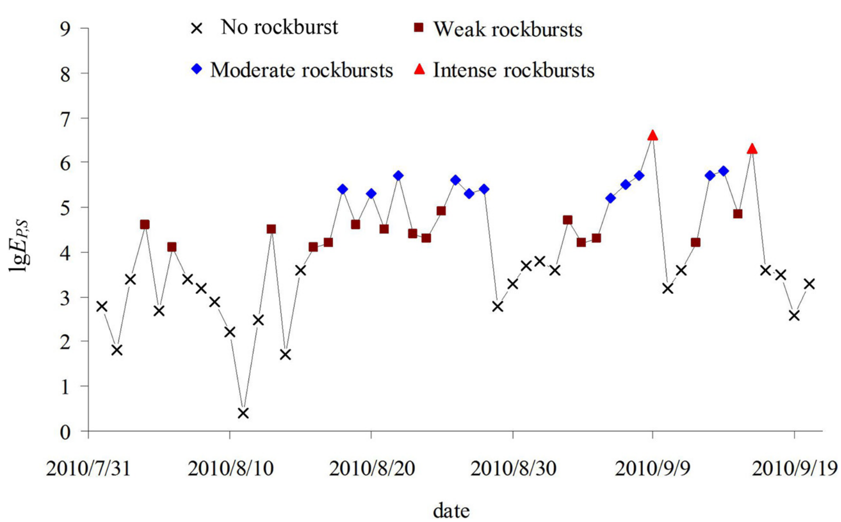

Fig. 7. Relationship between rockburst intensity and daily maximum-energy microseismic events during TBM excavation

during TBM excavation, when numerous weak and moderate rockbursts occur frequently within the same range, the excavation speed should be reduced to ensure that the stress and energy of the surrounding rock can be adjusted and released. At the same time, supporting measures should follow the working face closely.

Fig. 9 shows the energy distribution of microseismic events during TBM excavation in areas of rockbursts of different intensities (none, weak, moderate, and intense). It can be seen in Fig. 9 that the range of energies (logarithmic) of all microseismic events was between –1 and 7, primarily concentrated in the range of 1–5. The energy distribution of microseismic events during the evolution of rockbursts of different intensities is not same. The distribution range of the microseismic energy moves in the direction of high energy as the level of rockburst intensity increases (intense rockbursts > moderate rockbursts > weak rockbursts > no rockburst). The energy (logarithm) of microseismic events for intense rockbursts ranges from –1 to 7, that of moderate rockbursts ranges from –1 to 6, that of weak rockbursts ranges from –1 to 5, and that of no rockbursts ranges from –1 to 4.

Table 2. Occurrence Time and Energy Release (Logarithm) of a Typical Rockburst in Deep Tunnels of the Jinping II Hydropower Station

Date	Time (h:min:s)	Rockburst intensity	Energy release (logarithm)
Sep. 9	16:02:19	Intense	6.33
Sep. 12	11:23:42	Weak	4.21
Sep. 13	3:32:11	Moderate	5.72
Sep. 14	16:02:19	Moderate	5.80
Sep. 15	12:20:53	Weak	4.81
Sep. 16	14:08:07	Intense	6.62

Relationship between Microseismic Energy and Intensity of Immediate Rockburst during DBM Excavation

DBM excavation of drainage tunnel chainage SK4+810~5+196 (Fig. 2) has the same geological conditions and overburden depths

Date	Rockburst Intensity
5 Sep. 2010	No rockburst
6 Sep. 2010	⊕ ⊕ ⊕
7 Sep. 2010	⊕ ⊕ ⊕ ⊕ ⊙
8 Sep. 2010	⊕ ⊕ ⊕ ⊕ ⊕ ⊕ ⊙ ⊕ ⊕ ⊕ ⊕ ⊕
9 Sep. 2010	⊕ ⊕ ⊕ ⊙ ⊕ ◎

Note: All of the rockbursts are derived from the field monitoring, arranged in chronological order up to the occurrence. In Fig.8 ⊕ ⊙ ◎ represent weak, moderate, and intense rockbursts, respectively.

Fig. 8. Weak and moderate rockbursts before the intense rockburst on September 9, 2010

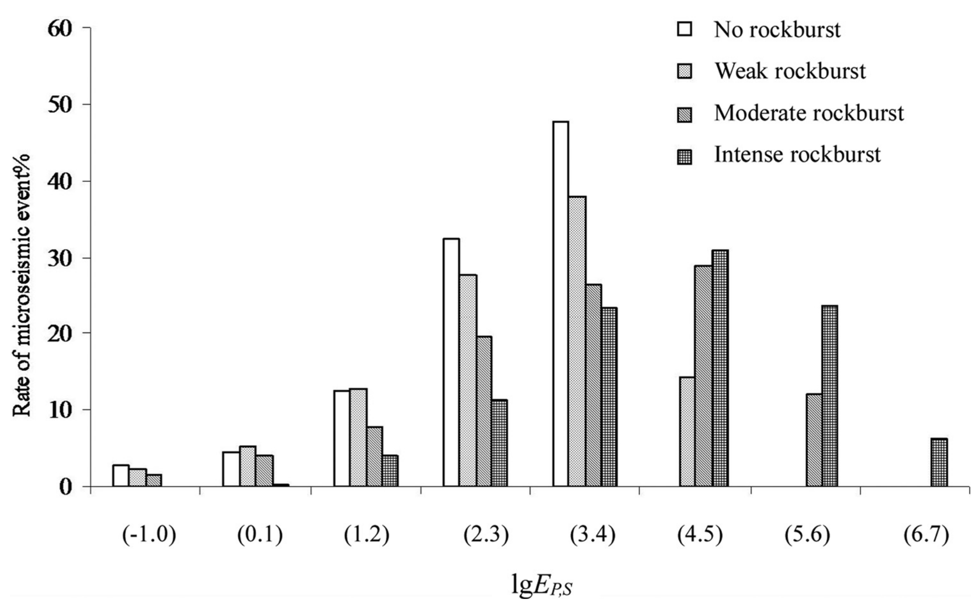

Fig. 9. Energy distribution of microseismic events in immediate rockbursts of different intensities during TBM excavation

as the TBM excavation. The relationship between rockburst intensity and maximum microseismic energy (logarithmic) in the DBM excavation has the same characteristics as in the TBM excavation: with intense rockbursts, >6; with moderate rockbursts, from 5 to 6; with weak rockbursts, from 4 to 5; and with no rockburst, <4, as shown in Fig. 10.

The occurrence of rockbursts in the four headrace tunnels and the drainage tunnel during DBM excavation indicates that all rockbursts occur singly. A large number of rockbursts that frequently occurred within the same range during TBM excavation was not found. The energy distribution of microseismic events for rockbursts of different intensities during DBM excavation is shown in Fig. 11. As seen in Fig. 11, the range of energies (logarithmic) of all microseismic events during the DBM excavation fell between –1 and 7 as well, concentrated in the range of –1 to 4. The energy distribution of microseismic events during the evolution of rockbursts of different intensities follows the same rule as that of TBM excavation (intense > moderate > weak > none).

Microseismic Energy Characteristics of Different Methods of Excavation

The microseismic energy (logarithmic) distribution of rockbursts of the same intensity is shown in Fig. 12 (all of the microseismic events during TBM and DBM excavation in the monitoring range are shown in Fig. 2). For rockbursts of the same intensity, the range of microseismic energy remained the same for either method of excavation: no rockbursts ranged from –1 to 4, weak rockbursts ranged from –1 to 5, moderate rockbursts ranged from –1 to 6, and intense rockbursts ranged from –1 to 7. The microseismic energy distribution under

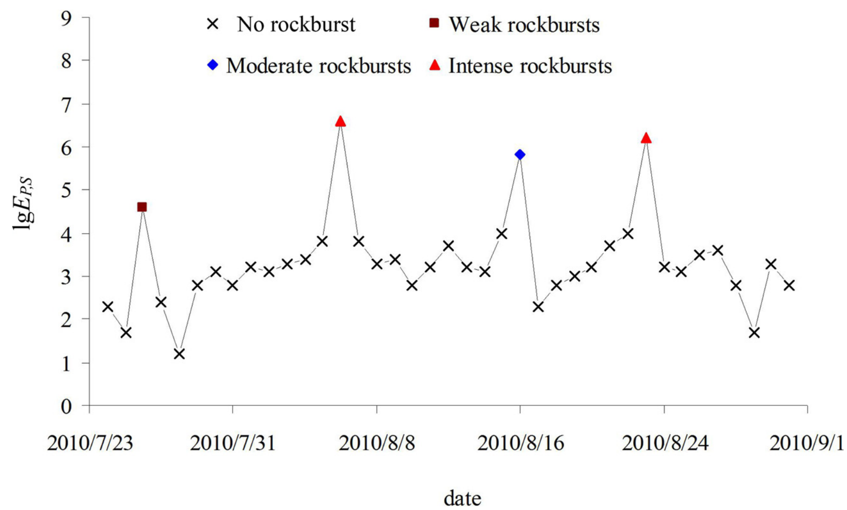

Fig. 10. Relationship between rockburst intensity and daily maximum-energy microseismic events during DBM excavation

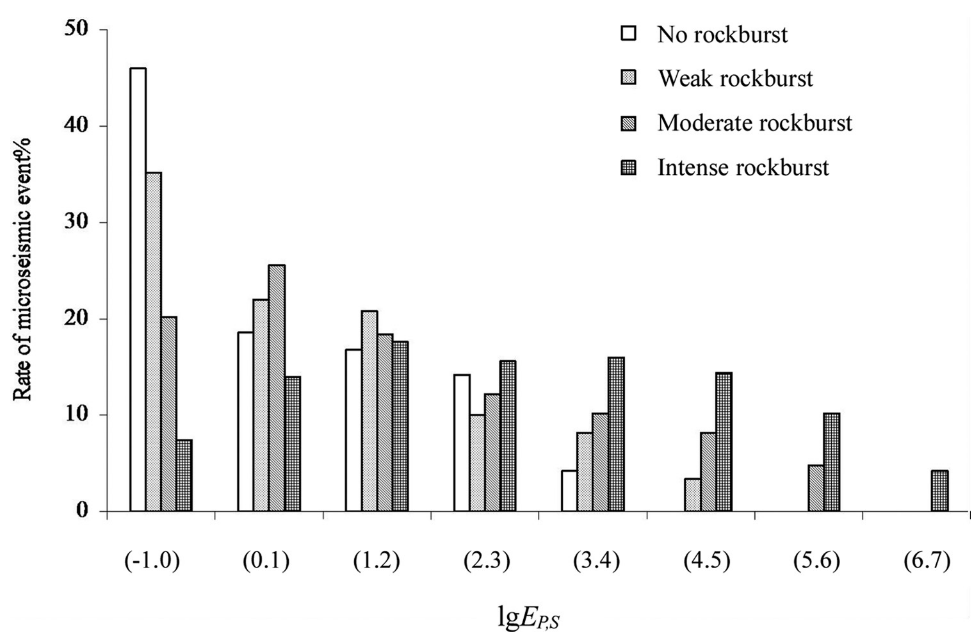

Fig. 11. Energy distribution of microseismic events in immediate rockbursts of different intensities during DBM excavation

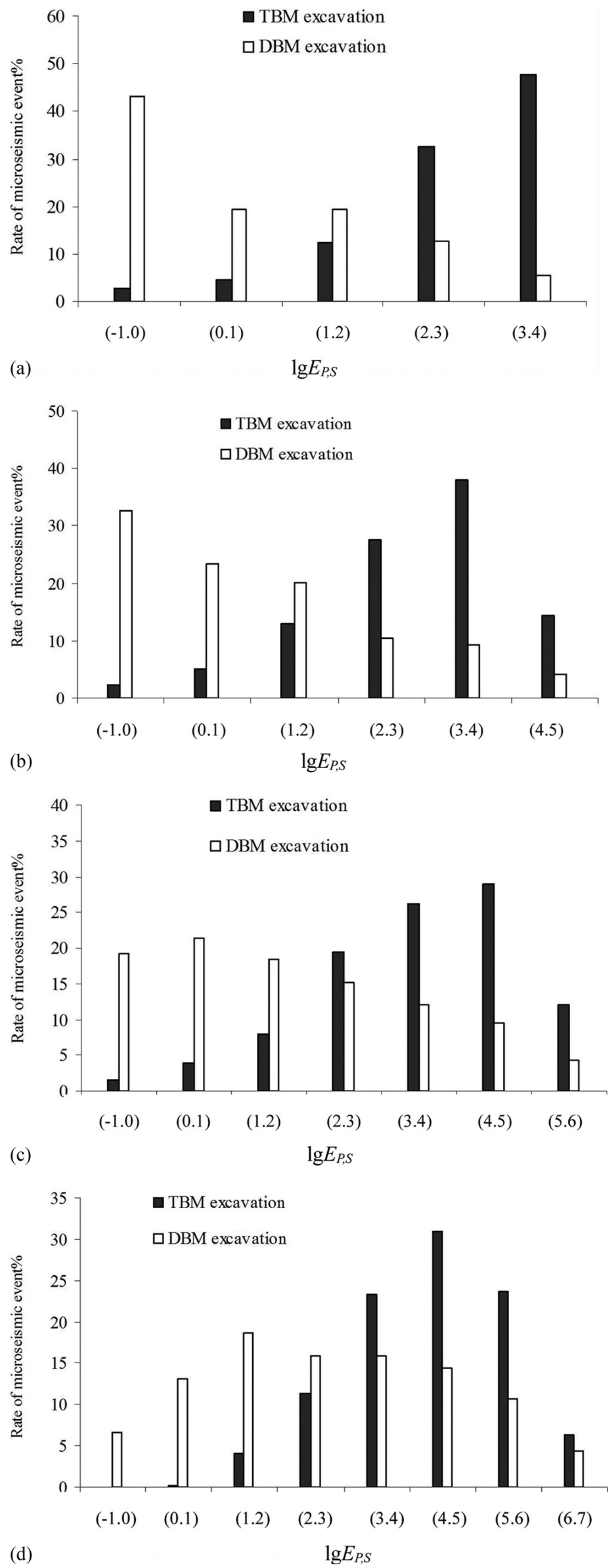

Fig. 12. Energy distribution of microseismic events in immediate rockbursts of different intensities during TBM and DBM excavation: (a) no rockburst; (b) weak rockbursts; (c) moderate rockbursts; (d) intense rockbursts

TBM excavation was higher than that under DBM. Figs. 12(a–d) also indicate that the energy distribution of microseismic events during the evolution of rockbursts of different rockburst intensities are not the same (intense rockbursts > moderate rockbursts > weak rockbursts > no rockburst).

In the evolution of processes of rockbursts of the same intensity during TBM and DBM excavation, the distribution range of microseismic energy was the same, but the concentration range differed (the microseismic energy of TBM excavation was larger than that of DBM). TBM excavation leads to static unloading, in which microseismic events are caused by the unloading process of the surrounding rock. The microseismic energy from TBM excavation was concentrated in the range of 10^1–10^5 J. The initial in-situ stress of the working face consists of dynamic unloading stress fields during DBM excavation. The integrality and bearing capacity of the surrounding rock are reduced by blasting effects. When combined with the impact of the microcracking caused by the blasting stress wave, microseismic energies from DBM excavation were concentrated in a range of $<10^4$ J. The concentration range with TBM excavation, then, was larger than that with DBM.

Analysis and Discussion

The relationship between the maximum energy microseismic events of the working face and the intensity of immediate rockbursts are the same in deep tunnels regardless of whether TBM or DBM excavation is used, as shown in the rockburst cases discussed earlier. Given this, it appears that microseismic energy can be used as a basis for estimating the immediate rockburst intensity.

TBM excavation involves static unloading, with which damage is to the local area. The bearing capacity and storage capacity of energy of the surrounding rock are greater than those of DBM excavation. In the evolution of intense rockbursts during the TBM excavation, the energy release by the surrounding rock takes place step by step (Barton 2000). Before the occurrence of intense rockbursts, a large number of weak and moderate rockbursts frequently occur in the range of the intense rockburst zone and increase with the evolution of intense rockbursts (Figs. 7 and 8). Initial in-situ stress of the working face during DBM excavation consists of dynamic unloading stress fields, where the area of damage is wide. The bearing capacity and storage capacity of energy of the surrounding rock are relatively poor (Read 2004). All of the rockbursts occur singly and completely release the elastic potential energy of the surrounding rock (Fig. 10).

The findings of this paper not only reveal the relationship between immediate rockbursts and microseismic energy but also provide an important guide for the establishment of a dynamic warning system to reduce the risk of rockbursts during different excavation methods. In addition to the authors' work on immediate rockbursts, investigation of time-delay rockbursts is necessary.

Conclusions

This paper investigates the microseismic energy in the evolutionary process of immediate rockbursts in deep tunnels at Jinping II Hydropower Station in Sichuan Province, China. The following conclusions are drawn:

1. The daily maximum energy of microseismic events of the working face can be used as a basis for estimating the immediate rockburst intensity.
2. In the evolutionary process of high-level rockbursts during TBM excavation, a large number of low-level rockbursts

frequently occur in the same range and increase with the evolutionary process of high-level rockbursts. This phenomenon was not found to occur during DBM excavation.

3. In the evolutionary processes of same-intensity rockbursts, microseismic energy has the same distribution range for each excavation method. The distribution range of microseismic energy moves in the direction of high energy as the level of rockburst intensity increases.
4. With TBM excavation, microseismic energy (concentrated in the range of 10^1–10^5 J) is higher than that with DBM excavation (concentrated in a range $<10^4$ J).

Acknowledgments

The authors acknowledge the financial support from National Key Technologies R&D Program of China under Grant 2013BAB02B01; the National Natural Science Foundation of China under Grant 51509092&51479192; the Fund of State Key Laboratory of Geomechanics and Geotechnical Engineering Grant Z015004; the Fund of Jiangxi Province (Grant 20161BAB216141); and funding from the Jiangxi Province Department of Education (Grant 150518). The original monitoring data were derived from State Key Laboratory of Geomechanics and Geotechnical Engineering Institute of Rock and Soil Mechanics, Chinese Academy of Sciences, Wuhan.

References

Abuov, M. G., Aitaliev, S. M., Ermekov, T. M., Zhanbyrbaev, N. B., and Kayupov, M. A. (1988). "Studies of the effect of dynamic processes during explosive break-out upon the roof of mining excavations." *J. Min. Sci.*, 24(6), 581–590.

Barton, N. (2000). *TBM tunneling in jointed and faulted rock*, Balkema, Rotterdam, Netherlands, 61–64.

Cai, M. (2008). "Influence of stress path on tunnel excavation response—Numerical tool selection and modeling strategy." *Tunnelling Underground Space Technol.*, 23(6), 618–628.

Chattopadhyay, A., Singh, A., and Dhua, S. (2014). "Effect of heterogeneity and reinforcement on propagation of a crack due to shear waves." *Int. J. Geomech.*, 10.1061/(ASCE)GM.1943-5622.0000356, 04014013.

Chen, B. R., Feng, X. T., Li, Q. P., Luo, R. Z., and Li, S. (2015). "Rock burst intensity classification based on the radiated energy with damage intensity at Jinping II Hydropower Station, China." *Rock Mech. Rock Eng.*, 48(1), 289–303.

Chen, B. R., Feng, X. T., and Ming, H. J. (2012). "Evolution law and mechanism of rockburst in deep tunnels: Time-delayed rockburst." *Chin. J. Rock Mech. Eng.*, 31(3), 561–569 (in Chinese).

Cook, M. A., Cook, U. D., and Clay, R. B. (1966). "Behavior of rock during blasting." *Trans. Soc. Min. Eng.*, 10(2), 17–25.

Eshragi, A., and Zare, S. (2015). "Face stability evaluation of a TBM-driven tunnel in heterogeneous soil using a probabilistic approach." *Int. J. Geomech.*, 10.1061/(ASCE)GM.1943-5622.0000452, 04014095.

Feng, G. L., Feng, X. T., Chen, B. R., Xiao, Y. X., and Jiang, Q. (2015). "Sectional velocity model for microseismic source location in tunnels." *Tunnelling Underground Space Technol.*, 45, 73–83.

Feng, X. T., Chen, B. R., and Zhang C. Q. (2013). *Mechanism warning and dynamic control of rockburst development processes*, China Social Sciences Publishing House, Beijing (in Chinese).

Feng, X. T., and Zhou, H. (2006). *Research report on stability of surrounding rock mass and structure design of diversion tunnels of Jinping II Hydropower Station at Yalong River during invite public bidding and design phase*, Institute of Rock and Soil Mechanics, Chinese Academy of Sciences, Wuhan, China.

He, M. C., Miao, J. L., and Feng, J. L. (2010). "Rock burst process of limestone and its acoustic emission characteristics under true-triaxial unloading conditions." *Int. J. Rock Mech. Min. Sci.*, 47(2), 286–298.

Li, T., Cai, M. F., and Cai, M. (2007). "A review of mining-induced seismicity in China." *Int. J. Rock Mech. Min. Sci.*, 44(8), 1149–1171.

Mendecki, A. J., Van Aswegen, G., and Mountfort, P. (1999). "A guide to routine seismic monitoring in mines." Chapter 1, *A handbook on rock engineering practice for tabular hard rock mines*, Safety in Mines Research Advisory Committee, Johannesburg, South Africa, 287–309.

Read, R. S. (2004). "20 years of excavation response studies at AECL's underground research laboratory." *Int. J. Rock Mech. Min. Sci.*, 41(8), 1251–1275.

Rutqvist, J., and Rinaldi, A. (2013). "Modeling ground deformations and potential for induced micro-seismicity at the In Salah CO_2 storage operation, Algeria." *Poromechanics V*, 10.1061/9780784412992.155, 1299–1308.

Savoikar, P., and Choudhury, D. (2012). "Translational seismic failure analysis of MSW landfills using pseudodynamic approach." *Int. J. Geomech.*, 10.1061/(ASCE)GM.1943-5622.0000127, 136–146.

Tang, B. Y. (2000). "Rockburst control using distress blasting." Ph.D. thesis, McGill Univ., Montreal.

Tang, S. H., Pan, Y., Huang, Y. H., and Ji, X. W. (2009). "Application research of microseismic monitoring technology to geostress hazards in deep mining." *Chin. J. Rock Mech. Eng.*, 28(S2), 3597–3603 (in Chinese).

Tang, Y. (1992). "A new classification of rockburst intensity." *Geol. Rev.*, 38(5), 439–443.

Wang, L. S., Li, T. B., and Xu, J. (1999). "Study on rockburst and its intensity classifies in the tunnel of Erlang Mountain road." *Road*, 2, 41–45.

Yan, P., Lu, W. B., and Chen, M. (2011). "In-situ test research on influence of excavation method on induced damage zone in deep tunnel." *Chin. J. Rock Mech. Eng.*, 30(6), 1097–1106 (in Chinese).

Zhang, C. Q., Feng, X. T., Zhou, H., Qiu, S. L., and Wu, W. P. (2012a). "Case histories of four extremely intense rockbursts in deep tunnels." *Rock Mech. Rock Eng.*, 45(3), 275–288.

Zhang, C. Q., Feng, X. T., Zhou, H., Qiu, S. L., and Wu, W. P. (2012b). "A top pilot tunnel preconditioning method for the prevention of extremely intense rockbursts in deep tunnels excavated by TBMs." *Rock Mech. Rock Eng.*, 45(3), 289–309.